

# Kinetic Evidence for Separate Site Catalysis by Pyruvate Phosphate Dikinase†

Sara H. Thrall and Debra Dunaway-Mariano\*

Department of Chemistry and Biochemistry, University of Maryland, College Park, Maryland 20742

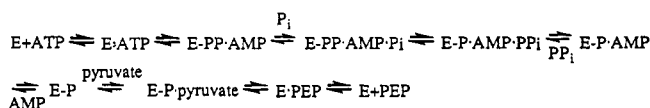
Received August 16, 1993; Revised Manuscript Received November 18, 1993\*

**ABSTRACT:** Pyruvate phosphate dikinase from *Clostridium symbiosum* catalyzes the interconversion of adenosine-5'-triphosphate (ATP), orthophosphate (P<sub>i</sub>), and pyruvate with adenosine 5'-monophosphate (AMP), inorganic pyrophosphate (PP<sub>i</sub>), and phosphoenolpyruvate (PEP) using a bi (ATP, P<sub>i</sub>) bi (AMP, PP<sub>i</sub>) uni (pyruvate) uni (PEP) kinetic mechanism and pyrophosphorylenzyme (E-PP) and phosphorylenzyme (E-P) covalent intermediates. The present studies were carried out to determine whether or not the site of catalysis of the E + ATP + P<sub>i</sub> ⇌ E-P + AMP + PP<sub>i</sub> partial reaction overlaps with that of the E-P + pyruvate ⇌ E + PEP partial reaction. Single-turnover experiments were carried out to test the effect of binding site occupancy on catalysis at a second site. Saturation of the enzyme with adenyl imidodiphosphate (AMPPNP) inhibited [<sup>32</sup>P]E-P formation from [β-<sup>32</sup>P]ATP and P<sub>i</sub> but did not significantly inhibit [<sup>32</sup>P]E-P formation from [<sup>32</sup>P]PEP. Likewise, saturation of E-P with AMP did not significantly inhibit [<sup>14</sup>C]PEP formation from [<sup>14</sup>C]pyruvate, suggesting separate, largely independent ATP/AMP vs pyruvate/PEP sites. Movement of the phosphorylhistidine residue between reaction sites was probed by testing oxalate as an inhibitor of phosphoryl transfer from E-P to [<sup>14</sup>C]pyruvate or to [<sup>14</sup>C]AMP. Both phosphoryl transfers were inhibited. These results were interpreted as evidence for the requirement for phosphorylhistidine release from the pyruvate site prior to participation in catalysis at the nucleotide site.

Pyruvate phosphate dikinase (PPDK)<sup>1</sup> from *Clostridium symbiosum* catalyzes the interconversion of ATP, P<sub>i</sub>, and pyruvate with AMP, PP<sub>i</sub>, and PEP by using a catalytic histidine residue to mediate the multiple phosphoryl transfer steps of the overall reaction (Scheme 1) [for reviews, see Wood et al. (1977) and Cooper and Kornberg (1974)]. The catalytic histidine first displaces AMP from the β-phosphoryl group of bound ATP, forming a pyrophosphorylated enzyme intermediate (E-PP). Two sequential phosphoryl transfers ensue, first, from the pyrophosphorylhistidine residue to P<sub>i</sub> to form PP<sub>i</sub>, and then from the resulting phosphorylhistidine residue to pyruvate to form PEP.

While the chemical steps of the PPDK-catalyzed reaction have been identified, the mechanism of the covalent catalysis is not yet known. In particular, the proximity of the substrate binding sites relative to the catalytic histidine and relative to one another has yet to be defined. The extent and manner of histidine movement between reaction sites also remains largely unexplored. The kinetic mechanism of the reaction (Scheme 1) would suggest that the ATP binding site and P<sub>i</sub> binding site are nonoverlapping (Wang et al., 1988; Thrall et al., 1993). Specifically, the E-PP-AMP complex formed in the reaction of enzyme with ATP does not release AMP prior to P<sub>i</sub> binding and reaction. The ping pong kinetics observed for the pyruvate/PEP segment of the reaction would, on the other hand, suggest the possibility of a common binding site for pyruvate/PEP and ATP/AMP or P<sub>i</sub>/PP<sub>i</sub> (Wang et al., 1988; Milner & Wood, 1976). However, on the basis of product inhibition (Milner & Wood, 1976) and chemical

Scheme 1: Kinetic Mechanism of the *Clostridium symbiosum* Pyruvate Phosphate Dikinase Catalyzed Reaction [from Thrall et al. (1993)]



modifications studies (Yoshida & Wood, 1978; Evans et al., 1980) Wood and co-workers have proposed three separate substrate binding/reaction sites.

The stereochemical course for phosphoryl transfer in the PPDK reaction provides further insight into the issue of catalysis at separate sites. Cook and Knowles (1985) demonstrated that transfer of the β-phosphoryl from chiral [β-<sup>18</sup>O, <sup>17</sup>O]ATP to pyruvate occurs with overall retention of stereochemistry. The β-phosphoryl group is first transferred to the histidine (to form E-PP) before it is transferred to pyruvate, and in order for the stereochemistry to be retained in the chiral [<sup>18</sup>O, <sup>17</sup>O]PEP formed, pyruvate must attack at the same face of the phosphoryl group of E-P from which AMP was displaced in the reaction of E-ATP → E-PP-AMP (see Scheme 2). This stereochemical arrangement could be met, as shown in Scheme 2, as a result of overlapping nucleotide and pyruvate binding sites or by rotational movement of the phosphorylated histidine between two separate sites.

The present studies were carried out to determine the extent to which the site of catalysis of the E + ATP + P<sub>i</sub> → E-P + AMP + PP<sub>i</sub> partial reaction overlaps with that of the E-P + pyruvate ⇌ E + PEP partial reaction. In this paper we present the results from pre-steady-state dead-end inhibition studies which suggest that the ATP/AMP and pyruvate/PEP binding sites are separate and that a conformational change within the protein links the two sites with the catalytic histidine.

## MATERIALS AND METHODS

**Materials.** The radioisotopes [<sup>32</sup>P]PP<sub>i</sub>, [γ-<sup>32</sup>P]ATP, [<sup>14</sup>C]-AMP, [<sup>14</sup>C]ATP, and [<sup>14</sup>C]pyruvate were purchased from

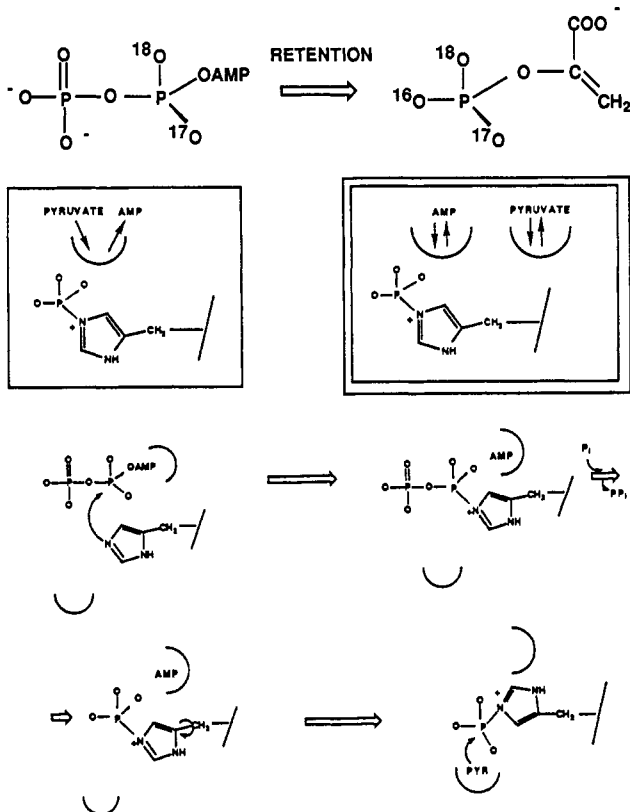
† This work supported by NIH Grant GM-36260.

\* To whom correspondence should be addressed.

• Abstract published in *Advance ACS Abstracts*, January 15, 1994.

<sup>1</sup> Abbreviations: PPDK, pyruvate phosphate dikinase; E-PP, pyrophosphorylenzyme; E-P, phosphorylenzyme; ATP, adenosine 5'-triphosphate; AMP, adenosine 5'-monophosphate; PEP, phosphoenolpyruvate; PP<sub>i</sub>, inorganic pyrophosphate; P<sub>i</sub>, inorganic phosphate; NADH, dihydronicotinamide adenine dinucleotide; Hepes, N-(2-hydroxyethyl)piperazine-N'-ethanesulfonic acid; LDH, lactate dehydrogenase; AMPPNP, adenyl imidodiphosphate.

Scheme 2: Retention of Phosphorus Stereochemistry as a Result of Catalysis at Overlapping vs Separate Reaction Sites



NEN Radiochemicals. All other chemicals were purchased from United States Biochemical Corp., Aldrich Chemicals, or Sigma. [ $\beta$ - $^{32}\text{P}$ ]ATP and [ $^{32}\text{P}$ ]PEP were prepared according to the method described in Carroll et al. (1989). A Beckman liquid scintillation counter (model LS 5801) was used for scintillation counting. The HPLC system used consisted of a Beckman 110A pump with a Beckman 420 controller attached to a Hitachi variable wavelength spectrophotometer. Spectrophotometric assays utilized a Gilford spectrophotometer model 250.

**PPDK Purification from *Escherichia coli*.** PPDK was purified, according to Pocalyko (1990), from *E. coli* JM101 cultures which were transfected with the plasmid pACYC184D12, which contains the PPDK gene.

**Rapid Quench Experiments.** All rapid quench experiments were performed at 25 °C using a rapid quench instrument from KinTek Instruments. A typical experiment entailed mixing a 43- $\mu\text{L}$  buffered solution containing enzyme, metal ion cofactors, and inhibitor with 43  $\mu\text{L}$  of buffered solution containing radiolabeled substrate. The reactions were quenched after a specified time with 164  $\mu\text{L}$  of 0.6 N HCl. The resulting solution was vortexed with 100  $\mu\text{L}$  of  $\text{CCl}_4$  to precipitate the protein and centrifuged to pellet the protein.

The  $^{14}\text{C}$ -labeled AMP and ATP present in the supernatant were separated by using a HPLC system consisting of a reverse-phase Beckman Ultrasphere C18 analytical column, eluted with an isocratic gradient of 25 mM  $\text{K}^+\text{P}_i$ , 2.5% triethylamine, and 5% methanol (pH 6.5), at a flow rate of 1 mL/min.  $^{14}\text{C}$ -labeled PEP and pyruvate present in the supernatant were separated by using an ion exchange Beckman Ultrasil HPLC column eluted with an isocratic gradient of 0.6 M KCl and 0.3 M  $\text{KH}_2\text{PO}_4$  (pH 5.0), at a flow rate 1 mL/min. For both HPLC separations, peaks were collected with a fraction collector (1 mL per fraction), and the fractions were counted by using liquid scintillation techniques.

The radiolabeled E-P and E-PP present in the  $\text{CCl}_4$  protein pellet were quantitated by dissolving the pellet (after removing excess solution on the pellet using a Kimwipe) in 500  $\mu\text{L}$  of 10 N  $\text{H}_2\text{SO}_4$ , at 100 °C for 1 min. A 100- $\mu\text{L}$  aliquot was assayed for radioisotope content by using liquid scintillation techniques.

The rate data were fit with a nonlinear least-squares fitting program (with Macintosh Kaleidagraph) to the equation for the first-order exponential increase of product (P) with time ( $t$ ):  $[\text{P}]_t = [\text{P}]_0(1 - e^{-kt})$ . Alternatively, the data were fit by curve simulation using the KINSIM program (Barshop et al., 1993), the kinetic mechanism of Scheme 1, the rate constants reported by Mehl et al. (1993), and the reactant/enzyme concentrations used in the experiment.

**Formation of Phosphorylated Enzyme (E-P).** E-P was formed by reacting PPDK and excess PEP in the presence of NADH and LDH. A typical reaction contained a 5.6-mL solution of 50 mM  $\text{K}^+\text{Hepes}$  (pH 7.0), 100  $\mu\text{M}$  PPDK (50 mg; based on MW 90 000), 5 mM  $\text{MgCl}_2$ , 10 mM  $\text{NH}_4\text{Cl}$ , 400  $\mu\text{M}$  NADH, and 0.5 unit of LDH. The reaction was initiated by the addition of PEP (200  $\mu\text{M}$ ). The decrease in absorbance of the reaction solution observed at 340 nm upon PEP addition corresponded to the reduction of 100  $\mu\text{M}$  pyruvate to lactate, and the production of 100  $\mu\text{M}$  E-P. E-P was isolated by loading the reaction mixture on a Sephadex G-75 column (1  $\times$  30 cm) and eluting it with 50 mM  $\text{K}^+\text{Hepes}$  (pH 7.0). One-milliliter fractions were collected and assayed for protein by measuring absorbance at 280 nm. All fractions containing E-P were combined and concentrated to a final enzyme concentration of  $\sim 50$  mg/mL with an Amicon Ultrafiltration Cell concentrating apparatus.

## RESULTS AND DISCUSSION

At the outset of these studies three models of PPDK binding and catalysis, each consistent with the reaction mechanism of Scheme 1 (Thrall et al., 1993) and the stereochemical course of the reaction (Cook & Knowles, 1985), were considered. In the first model, the pyruvate/PEP and ATP/AMP binding sites were assumed to be overlapping so that movement of the catalytic histidine between sites is not required and binding of one substrate would necessarily obstruct the binding of the substrate of the other partial reaction (Scheme 2). For the second model, the ATP/AMP and pyruvate/PEP binding sites were considered physically separate yet kinetically linked. In other words, occupancy at one site would affect catalysis at the other site. The third model assumed nonoverlapping, noninteracting sites.

Single-turnover experiments using rapid quench techniques were then employed to test the extent to which the substrate binding/reaction sites (ATP/AMP vs pyruvate/PEP) function independently of one another. These experiments entailed preincubating the enzyme with saturating amounts of a substrate (or an inert substrate analog) from one partial reaction and then observing the pre-steady-state reaction of the enzyme complex with a reactive substrate of the other partial reaction. Dead-end inhibition would evidence interacting sites, while no inhibition would evidence independent sites.

In the first experiment, PPDK (80  $\mu\text{M}$ ) was saturated with the inert ATP analog AMPPNP (1 mM) ( $K_d = 50$   $\mu\text{M}$ ; Mehl et al., 1994), and the resulting E-AMPPNP complex (40  $\mu\text{M}$  after mixing) was mixed with [ $^{32}\text{P}$ ]PEP (20  $\mu\text{M}$  after mixing) in a rapid quench instrument. The single-turnover time courses for the formation of  $^{32}\text{P}$ -labeled E-P from free enzyme or enzyme saturated with AMPPNP (eq 1) are shown in Figure 1. These data were fit with a nonlinear least-squares fitting

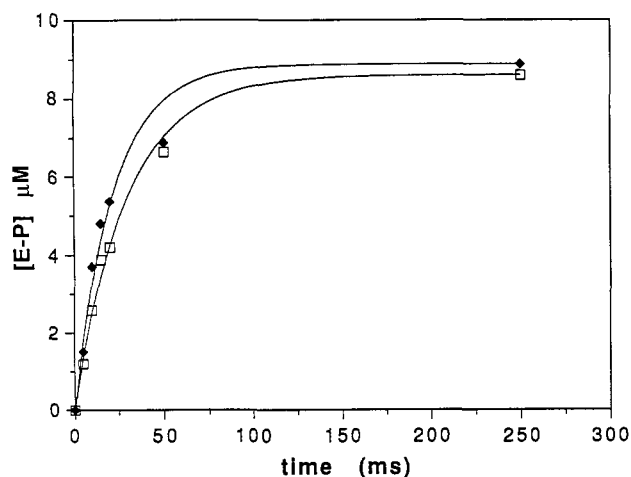
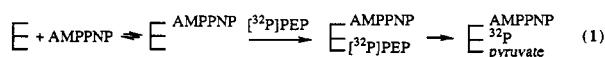
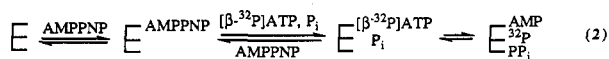


FIGURE 1: Single-turnover time course for the reaction of  $[^{32}\text{P}]\text{PEP}$  with  $\text{Mg}^{2+}/\text{NH}_4^+$ -activated PPDK and AMPPNP at 25 °C. The initial reaction mixture contained 40  $\mu\text{M}$  PPDK (subunit MW 90 000), 5 mM  $\text{MgCl}_2$ , 10 mM  $\text{NH}_4\text{Cl}$ , 50 mM  $\text{K}^+\text{Hepes}$  (pH 7.0), and 20  $\mu\text{M}$   $[^{32}\text{P}]\text{PEP}$ : ( $\blacklozenge$ ) 0  $\mu\text{M}$  AMPPNP, ( $\square$ ) 500  $\mu\text{M}$  AMPPNP.



program to the equation for the first-order exponential increase of product with time:  $P_t = [P]_0(1 - e^{-kt})$ . The first-order rate constants obtained for E-P formation in the absence and presence of AMPPNP are  $45 \pm 4$  and  $34 \pm 4 \text{ s}^{-1}$ , respectively.

As a control experiment, to ensure that AMPPNP is saturating the PPDK ATP binding site under the reaction conditions used for the inhibition experiment of Figure 1, single-turnover time courses were measured for the reaction of PPDK,  $[\beta\text{-}^{32}\text{P}]\text{ATP}$ , and  $\text{P}_i$  to form  $[^{32}\text{P}]\text{E-P}$  in the presence and absence of 500  $\mu\text{M}$  AMPPNP (eq 2).



The results, presented in Figure 2, show that AMPPNP inhibits formation of  $^{32}\text{P}$ -labeled E-P from reaction of PPDK with  $[\beta\text{-}^{32}\text{P}]\text{ATP}$  and  $\text{P}_i$ . The rate data were fit to simulated profiles of the reaction (Figure 2) generated with the kinetic fitting program KINSIM, the rates constants reported by Mehl et al. (1994), and the concentrations of reactants listed in the figure legend. The curve simulated for the reaction profile measured in the presence of 500  $\mu\text{M}$  AMPPNP was generated by including the AMPPNP binding step to the kinetic equation and assuming a  $K_d$  of 80  $\mu\text{M}$  for E-AMPPNP, which is close to the  $K_d$  of 50  $\mu\text{M}$  obtained by equilibrium dialysis measurements (Mehl et al., 1994). Together, Figures 1 and 2 demonstrate that saturation of the nucleotide site of PPDK with the inert ATP analog AMPPNP inhibits the pre-steady-state reaction of ATP and  $\text{P}_i$  with PPDK, but it has minimal effect on catalysis at the PEP/pyruvate site.

The second experiment was designed to test the comparative rates of  $[^{14}\text{C}]\text{PEP}$  formation from the reaction of  $[^{14}\text{C}]\text{pyruvate}$  with E-P and from the reaction  $[^{14}\text{C}]\text{pyruvate}$  with E-P-AMP (eq 3). Since we observed that incubation of E-P with AMP



over long time periods leads to ADP formation, the reaction was carried out by mixing E-P (160  $\mu\text{M}$ ) with a buffered solution of  $[^{14}\text{C}]\text{pyruvate}$  alone or of a mixture of  $[^{14}\text{C}]\text{pyruvate}$  and AMP. Previous studies had shown comparable  $k_{\text{on}}$  values

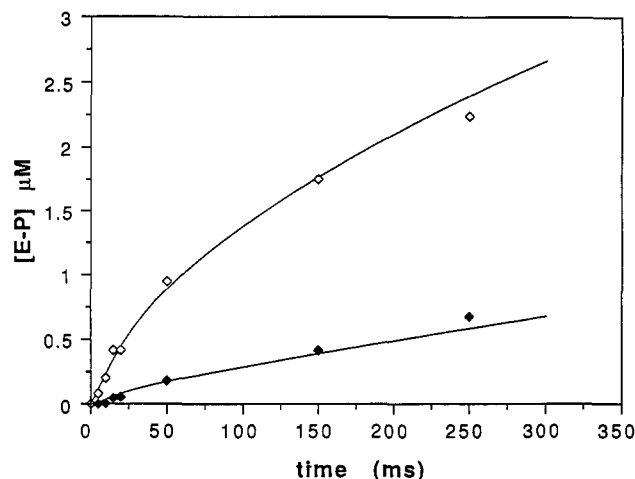


FIGURE 2: Single-turnover time course for the reaction of  $[\beta\text{-}^{32}\text{P}]\text{-ATP}$  with  $\text{Mg}^{2+}/\text{NH}_4^+$ -activated PPDK and AMPPNP at 25 °C. The initial reaction mixture contained 40  $\mu\text{M}$  PPDK (subunit MW 90 000), 5 mM  $\text{MgCl}_2$ , 10 mM  $\text{NH}_4\text{Cl}$ , 50 mM  $\text{K}^+\text{Hepes}$  (pH 7.0), 5  $\mu\text{M}$   $[\beta\text{-}^{32}\text{P}]\text{ATP}$ , and 20 mM  $\text{KH}_2\text{PO}_4$ : ( $\diamond$ ) 0  $\mu\text{M}$  AMPPNP, ( $\blacklozenge$ ) 500  $\mu\text{M}$  AMPPNP.

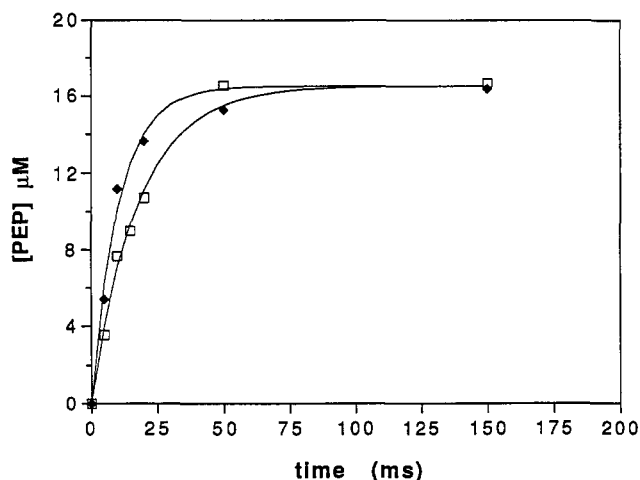
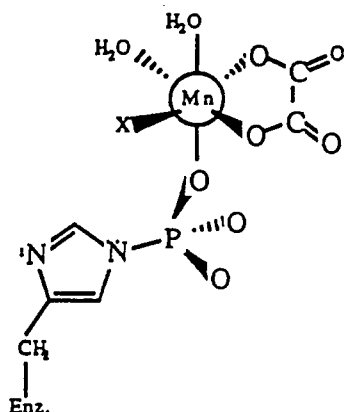


FIGURE 3: Single-turnover time course for a single turnover of  $[^{14}\text{C}]\text{-pyruvate}$  plus AMP with  $\text{Mg}^{2+}/\text{NH}_4^+$ -activated phosphorylated PPDK at 25 °C. The initial reaction mixture contained 160  $\mu\text{M}$  E-P (subunit MW 90 000), 5 mM  $\text{MgCl}_2$ , 10 mM  $\text{NH}_4\text{Cl}$ , 50 mM  $\text{K}^+\text{Hepes}$  (pH 7.0), and 33  $\mu\text{M}$   $[^{14}\text{C}]\text{pyruvate}$ : ( $\blacklozenge$ ) 0 mM AMP, ( $\square$ ) 10 mM AMP.

for AMP ( $3 \mu\text{M}^{-1} \text{ s}^{-1}$ ) and pyruvate ( $1 \mu\text{M}^{-1} \text{ s}^{-1}$ ) (Mehl et al., 1994), and therefore, by using the AMP (10 mM) in 300-fold excess to  $[^{14}\text{C}]\text{pyruvate}$  (33  $\mu\text{M}$ ), rapid occupancy of the nucleotide site was ensured. The time courses for single turnover reactions of E-P-AMP and E-P with  $[^{14}\text{C}]\text{pyruvate}$  are shown in Figure 3. The first-order rate constants calculated from these data are  $94 \pm 8 \text{ s}^{-1}$  for  $[^{14}\text{C}]\text{PEP}$  formation in the absence of AMP and  $56 \pm 3 \text{ s}^{-1}$  for  $[^{14}\text{C}]\text{PEP}$  formation in the presence of 10 mM AMP. Thus, only a small level of inhibition of PEP formation in the presence of saturating AMP ( $K_d = 70 \mu\text{M}$ ; Mehl et al., 1994) was observed, which suggests that the PEP and AMP sites on E-P are nonoverlapping.<sup>2</sup> The results from these first two experiments, together, provide evidence that the ATP/AMP and pyruvate/PEP binding sites are nonoverlapping and largely noninteracting sites and that the rate of movement of the catalytic histidine between these sites is fast relative to the time scale of the single-turnover experiment.

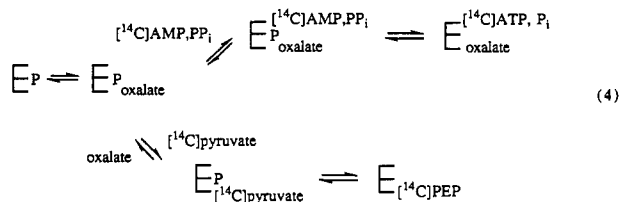
<sup>2</sup> This experiment does not rule out, however, the possibility that the E-P-AMP-PP<sub>i</sub> and E-P-pyruvate complexes assume kinetically distinct protein conformations.

Scheme 3: Metal Coordination Scheme within the E-P-Mn-oxalate Complex Adapted from Kofron et al. (1988)



The next set of experiments was designed to probe histidine movement between reaction sites by testing whether anchoring of the phosphohistidine residue at the pyruvate/PEP site interferes with catalysis at the ATP/AMP site. Previous studies (Michaels et al., 1975) had demonstrated that oxalate binds tightly to E-P, and sulfhydryl modification studies (Michaels et al., 1978) and limited proteolysis studies (Carroll, 1991) had indicated that the binding of oxalate to E-P induces a noticeable conformational change in the protein. Furthermore,  $\text{Mn}^{2+}/^{17}\text{O}$ -EPR studies (Kofron et al., 1988) of the E-P-Mn-oxalate complex have revealed, as illustrated in Scheme 3, coordination of both the oxalate and the phosphoryl group of the phosphohistidine residue to the metal cofactor. Thus, in this E-P-Mn-pyruvate enol(ate) analog complex, the phosphorylhistidine residue appears to be tightly anchored at the pyruvate/PEP binding site via the metal ion. We would therefore predict that if reaction at the nucleotide site requires release of the catalytic histidine from the pyruvate/PEP site, oxalate bound at the pyruvate site on E-P would inhibit phosphoryl transfer from E-P to AMP at the nucleotide site, provided that release of the catalytic histidine is slow relative to catalysis at the ATP/AMP site.

Accordingly, experiments were carried out to determine the effect of saturating the pyruvate binding site with oxalate on the pre-steady-state reaction of E-P with pyruvate to form PEP vs reaction of E-P with AMP and  $\text{PP}_i$  to form ATP and  $\text{P}_i$  (eq 4).<sup>3</sup> First, however, the affinity of oxalate for the



substrate binding sites on the free enzyme was tested. Earlier studies had shown that oxalate binds to PPDK in the presence of  $\text{Mn}^{2+}$  with a  $K_d \geq 200 \mu\text{M}$  (Michaels et al., 1975). Single-turnover experiments with  $[\text{E-P}]$  (to form  $^{32}\text{P}$ -labeled E-P) or  $[\gamma\text{-}^{32}\text{P}]\text{ATP}$  (to form  $^{32}\text{P}$ -labeled E-PP) and E-Mn<sup>2+</sup> in the presence or absence of 5 mM oxalate were carried out ( $\text{Mn}^{2+}$  was used in place of  $\text{Mg}^{2+}$  in order to optimize the level of E-PP formed from the  $[\gamma\text{-}^{32}\text{P}]\text{ATP}$ ; Thrall et al., 1993). The

<sup>3</sup> Equation 4 depicts nucleotide binding to the E-P-oxalate complex simply for convenience. We in fact do not know whether or not the oxalate must dissociate before the nucleotide binds to the phosphoryl-enzyme.

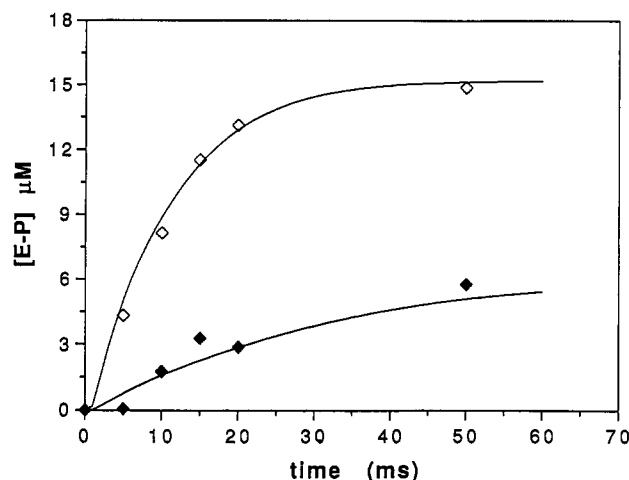


FIGURE 4: Single-turnover time course for the reaction of  $[\text{E-P}]$  with  $\text{Mn}^{2+}/\text{NH}_4^+$ -activated PPDK and oxalate at  $25^\circ\text{C}$ . The initial reaction mixture contained  $40 \mu\text{M}$  PPDK (subunit MW 90 000),  $10 \text{ mM}$   $\text{NH}_4\text{Cl}$ ,  $50 \text{ mM}$   $\text{K}^+\text{Hepes}$  (pH 7.0), and  $80 \mu\text{M}$   $[\text{E-P}]$ : (◇)  $5 \text{ mM}$  oxalate,  $2 \text{ mM}$   $\text{MnCl}_2$ , (◆)  $5 \text{ mM}$  oxalate,  $7 \text{ mM}$   $\text{MnCl}_2$ .

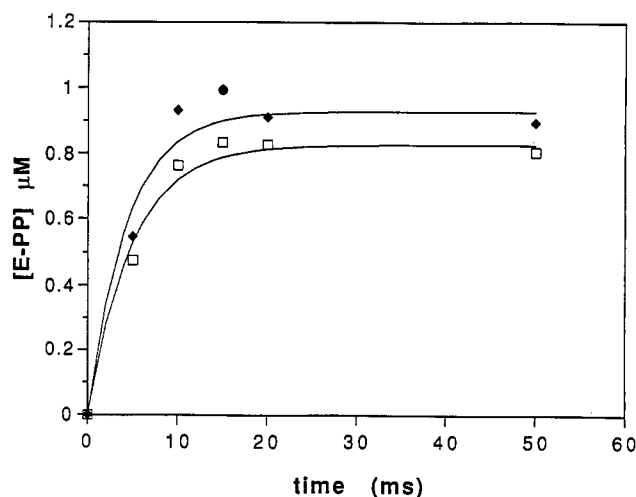


FIGURE 5: Single-turnover time course for the reaction of  $\gamma\text{-}[\text{E-PP}]$ -ATP with  $\text{Mn}^{2+}/\text{NH}_4^+$ -activated PPDK plus oxalate at  $25^\circ\text{C}$ . The initial reaction mixture contained  $40 \mu\text{M}$  PPDK (subunit MW 90 000),  $10 \text{ mM}$   $\text{NH}_4\text{Cl}$ ,  $50 \text{ mM}$   $\text{K}^+\text{Hepes}$  (pH 7.0), and  $1.5 \mu\text{M}$   $[\gamma\text{-}^{32}\text{P}]\text{ATP}$ : (◆)  $0 \mu\text{M}$  oxalate,  $2 \text{ mM}$   $\text{MnCl}_2$ , (□)  $5 \text{ mM}$  oxalate,  $7 \text{ mM}$   $\text{MnCl}_2$ .

results obtained are shown in Figures 4 and 5. The simulated curves shown in Figure 4 were generated with KINSIM using the rate constants reported in Mehl et al. (1994) and the reactant concentrations given in the figure legends and by assuming a  $K_d$  for E-oxalate of  $700 \mu\text{M}$ . Because oxalate binds  $\text{Mn}^{2+}$ , the  $[\text{Mn}^{2+}]$  used in the experiments was  $2 \text{ mM}$  in the absence of oxalate and  $7 \text{ mM}$  in the presence of the oxalate ( $5 \text{ mM}$ ). The rate profiles of Figure 5, which reflect no binding of oxalate at the ATP site, were fit to an exponential equation to obtain a first-order rate constant of  $230 \text{ s}^{-1}$  for both profiles. Oxalate thus binds weakly to the pyruvate site in E and not at all (within our limit of detection) to the nucleotide site in E.

Rapid quench analysis of  $[\text{E-P}]$  formation from E-P and  $[\text{E-P}]$ pyruvate in the presence of 0, 60, and  $120 \mu\text{M}$  oxalate (Figure 6) shows inhibition of PEP production by oxalate. The data were fit to simulated curves generated by KINSIM using the rate constants listed in Mehl et al. (1994) and the

<sup>4</sup> The data measured at the high oxalate concentration carry greater error.

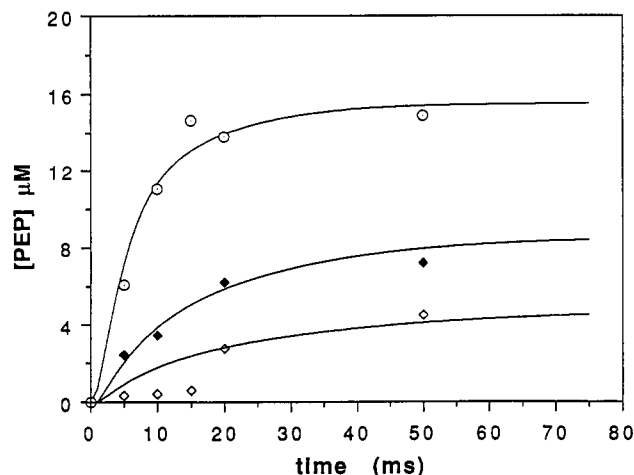


FIGURE 6: Single-turnover time course for the reaction of  $[^{14}\text{C}]$ -pyruvate with  $\text{Mg}^{2+}/\text{NH}_4^{+}$ -activated phosphorylated PPDK plus oxalate at  $25^\circ\text{C}$ . The initial reaction mixture contained  $160\ \mu\text{M}$  E-P (subunit MW 90 000),  $5\ \text{mM}$   $\text{MgCl}_2$ ,  $10\ \text{mM}$   $\text{NH}_4\text{Cl}$ ,  $50\ \text{mM}$   $\text{K}^+\text{Hepes}$  (pH 7.0), and  $33\ \mu\text{M}$   $[^{14}\text{C}]$ pyruvate: (○)  $0\ \mu\text{M}$  oxalate, (◆)  $60\ \mu\text{M}$  oxalate, (◇)  $120\ \mu\text{M}$  oxalate.

concentrations of E-P and pyruvate given in the figure legend. In the presence of  $60$  and  $120\ \mu\text{M}$  oxalate, the curves were generated by adding the oxalate binding step to the overall kinetic mechanism, and using initial concentrations of E-P, oxalate, and E-P-oxalate (after mixing and before reaction with pyruvate) as calculated from a E-P-oxalate  $K_d$  of  $0.1\ \mu\text{M}$ . The rate constant for oxalate binding was set to equal that of pyruvate ( $1.4\ \mu\text{M}^{-1}\text{s}^{-1}$ ; Mehl et al., 1994), and the corresponding off rate was then calculated (from the  $K_d$  of  $0.1\ \mu\text{M}$ ) as  $0.014\ \text{s}^{-1}$ . The pre-steady-state data indicate that oxalate binds to E-P- $\text{Mg}^{2+}$  more tightly ( $K_d = 0.1\ \mu\text{M}$ ) than had been previously observed for oxalate binding to E-P- $\text{Mn}^{2+}$  under steady-state conditions ( $K_d = 25\ \mu\text{M}$ ; Michaels et al., 1975).

Rapid quench experiments were then carried out to examine what effect, if any, oxalate has on the reaction of E-P with  $[^{14}\text{C}]\text{AMP}$  and  $\text{PP}_i$  to form  $[^{14}\text{C}]\text{ATP}$  (eq 4). E-P ( $40\ \mu\text{M}$ ) was preincubated with  $30\ \mu\text{M}$  oxalate and then mixed in the rapid quench with  $[^{14}\text{C}]\text{AMP}$  ( $6\ \mu\text{M}$ ) and  $\text{PP}_i$  ( $1\ \text{mM}$ ). The time course of  $[^{14}\text{C}]\text{ATP}$  formation shows that oxalate binding to the pyruvate site in E-P strongly inhibits reaction at the nucleotide site. The simulation shown in Figure 7 for the reaction in the presence of oxalate was generated by assuming a E-P-oxalate  $K_d = 0.035\ \mu\text{M}$  and the oxalate  $k_{\text{on}}$  and  $k_{\text{off}}$  equal to  $1.4\ \mu\text{M}^{-1}\text{s}^{-1}$  and  $0.046\ \text{s}^{-1}$ , respectively.<sup>5</sup>

**Conclusions.** Given that the ATP/AMP and pyruvate/PEP sites on the enzyme are nonoverlapping and the stereochemistry of the chiral  $\beta$ -phosphorus in  $[\beta\text{-}^{18}\text{O}, ^{17}\text{O}]\text{ATP}$  is retained in the chiral  $[\text{O}^{18}, \text{O}^{17}]\text{PEP}$  product (Cook & Knowles, 1985), we propose that the phosphorylhistidine residue undergoes some form of rotational movement between reaction sites during catalysis (Scheme 2). Presumably the movement of the histidine between sites occurs freely and rapidly since preincubation of enzyme with AMPNP does not impede its turnover of PEP. Only when the catalytic histidine is anchored to one site as it is in the tight E-P- $\text{Mg}^{2+}$ -oxalate or E-P- $\text{Mn}^{2+}$ -oxalate complex is reaction at the separate nucleotide site retarded. At the present, the

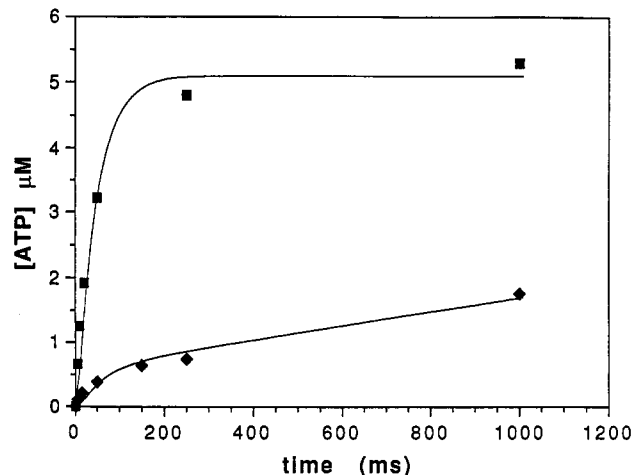


FIGURE 7: Single-turnover time course for the reaction of  $[^{14}\text{C}]\text{-AMP}$  and  $\text{PP}_i$  with  $\text{Mg}^{2+}/\text{NH}_4^{+}$ -activated phosphorylated PPDK plus oxalate at  $25^\circ\text{C}$ . The initial reaction mixture contained  $40\ \mu\text{M}$  E-P (subunit MW 90 000),  $5\ \text{mM}$   $\text{MgCl}_2$ ,  $10\ \text{mM}$   $\text{NH}_4\text{Cl}$ ,  $50\ \text{mM}$   $\text{K}^+\text{Hepes}$  (pH 7.0),  $1\ \text{mM}$   $\text{PP}_i$ , and  $6\ \mu\text{M}$   $[^{14}\text{C}]\text{AMP}$ : (■)  $0\ \mu\text{M}$  oxalate, (◆)  $30\ \mu\text{M}$  oxalate.

type of protein motion involved in translocation of the histidine between reaction sites during turnover is unknown, but studies of the shuttling mechanism are now in progress.

Finally, in view of the fact that the PPDK substrate binding sites are separate, the covalent catalysis used by this enzyme does not appear to have been linked to the conservation of binding sites during the evolution of this protein (Frey, 1992). Rather, the use of covalent catalysis must be related to the complexity of the overall reaction catalyzed and/or to the origin of the protein (Pacolyko et al., 1990).

## REFERENCES

- Barshop, B. A., Wrenn, R. F., & Frieden, C. (1983) *Anal. Biochem.* **130**, 134.
- Carroll, L. J. (1991) Ph.D. Thesis, University of Maryland, College Park, MD.
- Carroll, L. J., Mehl, A. F., & Dunaway-Mariano, D. (1989) *J. Am. Chem. Soc.* **111**, 5965.
- Cook, A. G., & Knowles, J. R. (1985) *Biochemistry* **24**, 51.
- Cooper, A. G., & Kornberg, H. L. (1974) *The Enzymes* (Boyer, P., Ed.) 3rd ed., Vol. 10, p 631, Academic Press, New York.
- Evans, C. T., Goss, N. H., & Wood, H. G. (1980) *Biochemistry* **19**, 5809.
- Frey, P. A. (1992) *The Enzymes* (Sigman, D. S., Ed.) Vol. XX, p 142–183, Academic Press, New York.
- Kofron, J. L., Ash, D. E., & Reed, G. H. (1988) *Biochemistry* **27**, 4781.
- Mehl, A. F., Xu, Y., & Dunaway-Mariano (1994) *Biochemistry* (preceding paper in this issue).
- Michaels, G., Milner, Y., & Reed, G. H. (1975) *Biochemistry* **14**, 3213.
- Michaels, G., Milner, Y., Moskovitz, B. R., & Wood, H. G. (1978) *J. Biol. Chem.* **253**, 7656.
- Milner, Y., & Wood, H. G. (1976) *J. Biol. Chem.* **251**, 7920.
- Pacolyko, D. J. (1990) Ph.D. Thesis, University of Maryland, College Park, MD.
- Thrall, S. H., Mehl, A. F., Carroll, L. J., & Dunaway-Mariano, D. (1993) *Biochemistry* **32**, 1803.
- Wang, H. C., Ciskanik, L., von der Saal, W., Villafranca, J. J., & Dunaway-Mariano, D. (1988) *Biochemistry* **27**, 625.
- Wood, H. G., O'Brien, W. E., & Michaels, G. (1977) *Adv. Enzymol. Relat. Areas Mol. Biol.* **45**, 85.
- Yoshida, H., & Wood, H. G. (1978) *J. Biol. Chem.* **253**, 7650.

<sup>5</sup> The biphasic appearance of the progress curve of inhibited enzyme presumably derives from fast reaction a population of uninhibited enzyme and slow reaction (as a result of slow release of oxalate or a slow conformational change) of a larger population of inhibited enzyme.